488 *Macromolecules* **2010**, *43*, 488–493
DOI: 10.1021/ma9019009

Macromolecules
ARTICLE

Evaluation of Topological Defects in Tetra-PEG Gels

Yuki Akagi,[†] Takuro Matsunaga,[‡] Mitsuhiro Shibayama,[‡] Ung-il Chung,[†] and Takamasa Sakai*,[†]

[†]*Department of Bioengineering, School of Engineering, The University of Tokyo, 7-3-1 Hongo, Bunkyo-ku, Tokyo 113-8656, Japan and* [‡]*Institute for Solid State Physics, The University of Tokyo, 5-1-5 Kashiwanoha, Kashiwa, Chiba 277-8581, Japan*

Received August 27, 2009; Revised Manuscript Received November 16, 2009

ABSTRACT: We have investigated the topological defects in the Tetra-PEG gel formed from two symmetrical tetra-arm polymers. The concentration of the elastically effective chains (EEC) was estimated from the elastic moduli and the reaction efficiency using the tree-like Miller-Macosko model. The concentration of EEC was in the range between the estimations of the affine and phantom theory. Furthermore, the formation of topological defects, especially entanglements and loops, was found to be negligible in the Tetra-PEG gel, which differs from other conventional model networks. This extremely homogeneous structure was formed due to the unique impenetrable sphere-like behavior of the tetra-arm star polymer in the semidilute solution and the unique symmetrical A−B type cross-end-coupling.

Introduction

Generally, polymer gels have inhomogeneities, because transient inhomogeneities in a gelling solution are frozen into the network during the cross-linking process. These frozen inhomogeneities are categorized into the spatial and topological inhomogeneities.[1] The ideal polymer network structure free from inhomogeneities has attracted a great deal of attention in the past few decades from both the engineering and scientific points of view. Aiming to form an ideal polymer network, many researchers developed "model networks" by using asymmetrical combination of monodispersed multifunctional molecules.[2−5] However, the obtained model networks did contain some inhomogeneities as elucidated by small angle neutron scattering (SANS), extracted sol fraction, elastic moduli, swelling degree, etc.,[6−8] or inhomogeneities were not investigated in detail. Recently, we designed and fabricated Tetra-PEG gel by A-B type "cross-end coupling" of two symmetrical tetra-arm star polymers of the same size.[9] The gel had high mechanical strength up to 10 MPa, comparable to native articular cartilage. The SANS result showed that practically no spatial inhomogeneities exist in the region, which is less than 200 nm in size.[10] Furthermore, the inhomogeneities did not appear even under the equilibrium swelling condition,[11] where spatial inhomogeneities are known to become obvious in other polymer gels.[12−14] It is speculated that this extremely homogeneous structure in tetra-PEG gels is due to the unique properties of the tetra-arm star polymers, which behave as impenetrable space-filled spheres in the semidilute solution. This situation is markedly different from that of the conventional model networks formed using linear polymers as building blocks; it is known that linear polymers interpenetrate each other in the semidilute regime.[15] The cross-linking process freezes these transient interpenetrations of polymers into permanent entanglements of the network. These permanent entanglements critically affect the network homogeneity. Because the permanent entanglements behave as pseudo-knots and divide the preprogrammed monodispersed mesh, mesh size inhomogeneities are introduced into the network. When the external load is applied to this network, the stress is concentrated in the vicinity of low-cross-link densities and/or on network defects, leading to the macroscopic fracture. In contrast, because the Tetra-PEG polymers behave as impenetrable space-filled spheres, it is expected that there are only a few entanglements frozen into the network. In this study, we investigated the topological inhomogeneities, i.e., the dangling chains, entanglements and loops, by measuring the reaction efficiency and the concentration of elastically effective chains (EEC).

Theoretical Section

The Miller Macosko (MM) theory was developed based on the recursive nature of the branching process and on elementary probability laws under three assumptions including (1) all functional groups of the same type are equally reactive, (2) all groups react independently of one another, and (3) no intramolecular reactions occur in finite species.[16] In order to apply this theory to the Tetra-PEG gel, we consider a stepwise copolymerization of tetra-functional monomers (A_4 and B_4). The probabilities that one of 4 arms leads out to a finite chain ($P(F_A{}^{out})$ and $P(F_B{}^{out})$) are presented as follows

$$P(F_A{}^{out}) = p_A P(F_B{}^{out})^3 + (1 - p_A) \quad (1)$$

$$P(F_B{}^{out}) = p_B P(F_A{}^{out})^3 + (1 - p_B) \quad (2)$$

where p_A and p_B are the reaction efficiency of the A and B groups, respectively. Here, we assume that p_A and $P(F_A{}^{out})$ are equal to p_B and $P(F_B{}^{out})$, respectively, because equimolar A_4 and B_4 species were used in this study. Thus, we are able to reduce this system to a stepwise homopolymerization of A_4. Equations 1 and 2 are reduced to

$$P(F^{out}) = pP(F^{out})^3 + (1 - p) \quad (3)$$

where p and $P(F^{out})$ are the reaction efficiency and the probability that one of 4 arms leads out to a "finite" chain, respectively. Thus,

*To whom correspondence should be addressed.

 Published on Web 12/09/2009

$P(F^{out})$ can be represented as follows

$$P(F^{\text{out}}) = \left(\frac{1}{p}-\frac{3}{4}\right)^{1/2} - \frac{1}{2} \quad (4)$$

Using $P(F^{out})$, the post gelation properties, such as the probability that a given tetra-arm polymer is a connection degree of $n(P(X_n))$ can be calculated.

The probability that a given tetra-arm polymer belongs to the connection degree of $n(P(X_n))$ is represented as

$$P(X_n) = {}_4C_n P(F^{out})^{(4-n)}[1-P(F^{\text{out}})]^n \quad (5)$$

Here, it should be noted that only when the n is equal to or higher than 3, the connections become cross-links. Using eq 5, the probability that a given tetra-arm polymer is the extractable sol ($P(X_0) = \omega_{\text{sol}}$), the effective cross-link probability of degree 3 ($P(X_3)$), and the effective cross-link probability of degree 4 ($P(X_4)$) are calculated as follows,

$$\omega_{sol} = P(F^{\text{out}})^4 \quad (6)$$

$$P(X_3) = {}_4C_3 P(F^{\text{out}})[1-P(F^{\text{out}})]^3 \quad (7)$$

$$P(X_4) = [1-P(F^{\text{out}})]^4 \quad (8)$$

The concentrations of cross-links (μ) and of EEC (ν) are represented respectively as follows,

$$\mu = c(P(X_3)+P(X_4)) \quad (9)$$

$$\nu = c\left(\frac{3}{2}P(X_3)+2P(X_4)\right) \quad (10)$$

Here, c represents the molar concentration of the tetra-arm polymer in the unit volume of material. In the affine theory and the phantom theory, the elastic moduli (G) are represented respectively as

$$G_{\text{af}}{}^0 = \nu RT \quad (11)$$

$$G_{\text{ph}}{}^0 = (\nu-\mu)RT \quad (12)$$

where R is the gas constant, and T is the absolute temperature.[17,18] In the case that the network is formed at dilution state (ϕ_{ap}), and is measured at certain condition (ϕ_{obs}), the modulus (G) is represented as

$$G = \nu_{\text{dry}} RT \phi_{\text{ap}}{}^{2/3} \phi_{\text{obs}}{}^{1/3} \quad (13)$$

where ν_{dry} is the concentration of EEC in the unit volume of dry network ($\phi = 1$). In this study, we performed the stretching test for the specimen in as-prepared state, i.e. $\phi_{\text{ap}} = \phi_{\text{obs}} = \phi_0$. Therefore, the modulus is represented as

$$G = \nu_{\text{dry}} \phi_0 RT = \nu RT \quad (14)$$

where ν is the molar concentration of EEC in the unit volume of material. Additionally, a trapped entanglement is known to act as pseudocross-link of degree 4 contributing to the elasticity.[19] The concentration of elastically effective entanglement (ν_{ent}) is represented by

$$\nu_{ent} = \varepsilon T_e \quad (15)$$

$$T_{\text{e}} = [1-P(F^{\text{out}})^3]^4 \quad (16)$$

where ε is the concentration of entanglements and T_{e} is the probability that all four chain ends coming from an entanglement lead to an infinite network, i.e., the probability that an entanglement is trapped. Assuming the phantom-like behavior of trapped entanglement, the elastic moduli are represented by

$$G_{\text{af}} = (\nu+\nu_{\text{ent}})RT \quad (17)$$

$$G_{\text{ph}} = (\nu-\mu+\nu_{\text{ent}})RT \quad (18)$$

Experimental Section

Sample Preparation. Tetra-amine-terminated PEG (TAPEG) and tetra-NHS-glutarate-terminated PEG (TNPEG) were prepared from tetrahydroxyl-terminated PEG (THPEG) having equal arm lengths. Here, NHS stands for *N*-hydroxysuccinimide. The details of TAPEG and TNPEG preparation were reported previously.[9] The molecular weights (M_{w}) of TAPEG and TNPEG were matched to each other (M_{w} = 10 kg/mol). The activity of the functional group was estimated using NMR. Tetra-PEG gels were synthesized as follows. Constant amounts of TAPEG and TNPEG (40−140 mg/mL) were dissolved in phosphate buffer (pH7.4) and phosphate-citric acid buffer (pH5.8), respectively. The corresponding initial polymer volume fractions, ϕ_0, were in the range between 3.54×10^{-2} and 1.24×10^{-1} (mass density = 1.129 g/cm^3). In order to control the reaction rate, the ionic strengths of the buffers were chosen to be 25 mM for lower macromer concentrations (40−80 mg/mL) and 50 mM for higher macromer concentrations (100−140 mg/mL). Two solutions were mixed, and the resulting solution was poured into the mold. At least 12 h were allowed for the completion of the reaction before the following experiment was performed.

Measurement of Extractable Sol Fraction. The gel was fabricated in rectangular films (30 mm high, 5 mm wide, 2 mm thick). The obtained gels (approximately 3 g) were immersed in 150 mL of H_2O at 37 °C for 48 h with shaking. The extracted solution was concentrated to 10 mL, then freeze-dried. The total weight of the soluble components of the gel was measured. The element composition of the soluble component was measured using a thermogravimetry analyzer (TG/DTA 6200). More than three samples were tested for each network concentration.

Stretching Measurement. The stretching measurement was carried out on the rectangular films using a mechanical testing apparatus (Rheo Meter: CR-500DX-SII, Sun Scientific Co.) at a crosshead speed of 0.1 mm/s. The gel samples were used in as-prepared state. Each specimen was stretched and released repeatedly for 2 times and the reproducibility was confirmed. More than 10 samples were tested for each network concentration, and the observed moduli were arithmetically averaged.

Results and Discussion

Theoretical Description of the Gelation from Tetra-Arm Polymer. The calculation results of the MM theory are plotted in Figure 1. First, we estimated the gelation threshold, which is defined as the lowest value of p where eq 3 has a nontrivial solution with respect to p. The gelation point of tetra-arm polymer is estimated to be 1/3. As shown in Figure 1a, connections of lower degrees are stepwisely

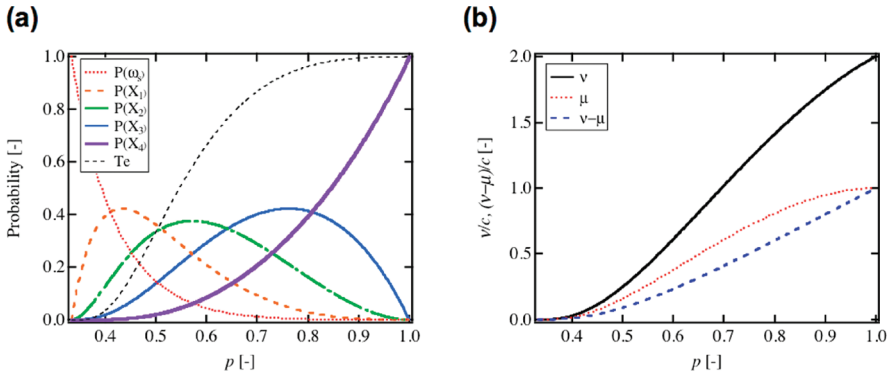

Figure 1. (a) Probabilities of the existence of X_n and T_e as a function of p. (b) ν and $\nu - \mu$ normalized by c as a function of p.

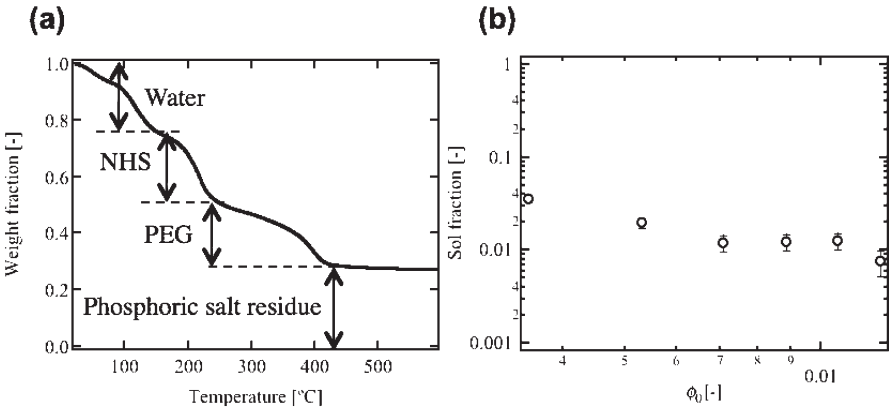

Figure 2. (a) Weight fraction of the extract as a function of the temperature. (b) Sol fraction as a function of ϕ_0.

converted into connections of higher degrees as the reaction proceeds. When the reaction proceeds stoichiometrically, all of the species are converted into connections of degree 4. Practically, we can obtain the $P(X_0)$ from the sol fraction extracted from the gel. Thus, the reaction efficiency (p) is estimated from eq 6. Using the value of p, we can estimate all of the values considered in this model for the specific gel samples. In order to obtain the elastic moduli, connections with degrees equal to or higher than 3 are considered, because $P(X_0)$, $P(X_1)$, and $P(X_2)$ are the probabilities of the sol fraction, dangling chain, and chain extender, respectively, none of which contribute to the elasticity. Thus, the elastic moduli of the network without considering the entanglements are calculated by eqs 11 and 12 using the values of $P(X_3)$ and $P(X_4)$ (Figure 1b).

Reaction Efficiency. In order to estimate the reaction efficiency, the weights of the extracts of the gels were measured. The extracts involved the polymers not connected to the infinite network (sol fraction), the NHS group disrupted from the polymers, and phosphoric salt used in the buffer solution. In order to measure the weight of the sol fraction, TGA experiments were performed. An example of the TGA results is shown in Figure 2a. The H_2O (including hydrated water of phosphate and citrate), NHS, and PEG were gasified around 100, 200, and 400 °C, respectively. From Figure 2a, we obtained the weight fraction of PEG in the extract. Using the weight fraction of the PEG and the total weight of the extract, we obtained the ω_{sol} (Figure 2b). The ω_{sol} seemed to decrease slightly with the feed polymer fraction (ϕ_0), and was on the order of 10^{-2}.

The p estimated from the ω_{sol} using eq 6 is shown in Figure 3 as a function of ϕ_0. The reaction efficiency increased

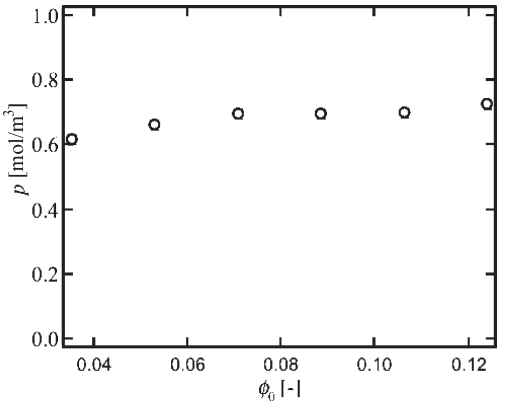

Figure 3. The reaction efficiency (p) as a function of ϕ_0.

as the ϕ_0 increased; however, the variation was small. This almost constant p can be accounted for using the SANS result of our previous study. In the concentration range measured in this study, the tetra-arm polymers behaved as impenetrable space-filled spheres. Thus, the probability of encountering the polymers is likely constant. As a result, the reaction efficiency of this cross-end coupling reaction was approximately up to $p = 0.75$. In other words, one of four arms could not find the neighboring connectable arms. This reaction efficiency is smaller than those of other model networks.[4,20] This seems to be an inherent defect in this system. This result can be interpreted as follows: first, the whole system loses macroscopic fluidity at the gelation threshold, which was set to several minutes using the buffer solution. Even at $p = 0.4$, more than half of the polymers

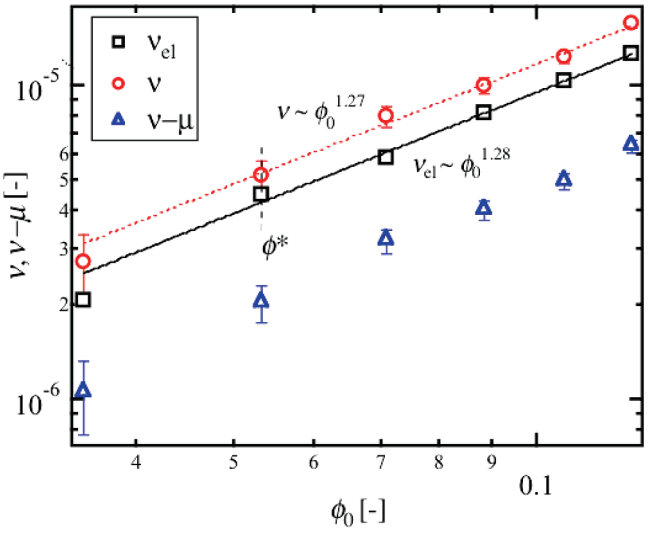

Figure 4. ν_{el} estimated from the elastic modulus, and the ν and $\nu - \mu$ estimated from the sol fraction as a function of ϕ_0.

connect to the infinite network as shown in Figure 1(a). Thus, long-range diffusion is unlikely to occur after the gelation threshold. In other words, mixing of the building blocks (i.e., Tetra-PEG chains) is not allowed after the gelation threshold. Second, at $p = 0.5$, almost all of the building blocks are connected to the infinite network. In the phantom theory, the diffusivity of the f-linked cross-link (X_f) becomes smaller as f increases, while the affine theory does not allow any diffusion for cross-links. The diffusivity of the reactive species was expected to decrease as the reaction proceeded. Thus, the conversion from X_3 to X_4 seems difficult to achieve. Because $p = 0.75$ in the region where X_3 is converted to X_4, the reaction might be terminated at this point.

Concentration of EEC. The elastic moduli were measured using a stretching measurement, and the concentration of EEC (ν_{el}) was estimated by eq 14. Figure 4 shows the ν_{el} as a function of ϕ_0. The fitting result (solid line) and the critical overlapping concentration (ϕ^*) of the tetra-arm polymer are also shown in Figure 4. In the region above the ϕ^*, ν_{el} increased in a power-law fashion, i.e., $\nu_{el} \sim \phi_0^{\beta}$, with $\beta_{el} = 1.28$. Generally, in other model network systems, ν_{el} increases with a higher exponent than unity, in many cases $\beta \approx 2$, of ϕ_0 in the concentrated region above the ϕ^*, because of the contribution of the entanglements (ν_{ent}) to the ν_{el}.[21] It is known that the molecular weight between two entanglements (M_e) of linear PEG in the bulk is 2200 and that the concentration of entanglements (ε) scales with ϕ_0 in the semidilute region as $\varepsilon \sim \phi_0^{9/4}$.[22,23] This is why the scaling exponent is higher than unity, i.e., $\nu_{ent} \sim \varepsilon \sim \phi_0^{9/4}$. Many researchers have reported an increase of the entanglement contribution with increasing network concentration in the semidilute region.[20,24] Even if a chain extender with a molecular weight smaller than M_e was used, the entanglement existed in the network, showing $\beta = 1.52$.[25] Thus, the entanglements are inevitable in networks when linear polymers are used as a building block. Considering the Tetra-PEG gel, the molecular weight of one arm of the tetra-arm polymer is 2500; i.e., the molecular weight of the polymer connecting the cross-links is 5000. Thus, the molecular weight of the arm is comparable to the length over which an entanglement occurs. However, the scaling exponent was near unity, suggesting that entanglements contribute only slightly to the elasticity of Tetra-PEG gel. In order to discuss the value of ν_{el}, we compared the ν_{el} with the values expected from the affine and phantom theories.

The values of ν and $\nu - \mu$ estimated from the reaction efficiency using eqs 9 and 10 are also displayed in Figure 4. The fitting result of ν (dashed line) is also shown in Figure 4. In the region above the ϕ^*, ν increased in a power-law fashion, i.e., $\nu \sim \phi_0^{\beta}$, with $\beta_{af} = 1.27$. It should be noted that ν, which represents the contribution of the chemical cross-link, had a higher exponent than unity, corresponding to the increase of p with increasing ϕ_0. Although ν_{el} was slightly smaller than ν, β_{el} was in good agreement with β_{af}. This result suggests two possible hypotheses: (i) The elasticity of Tetra-PEG gel is described by the affine theory and only a few entanglements exist. (ii) The elasticity of Tetra-PEG gel is described by the phantom theory and approximately μ entanglements exist ($\nu_{ent} = \mu$). Hypothesis ii has often been accepted in conventional model networks. However, hypothesis ii is unlikely in the Tetra-PEG gel for the following reasons. If the Tetra-PEG gel is described by phantom network theory, many entanglements exist, and ν_{el} should increase with a higher exponent, obeying the exponent of $\varepsilon \sim \phi_0^{9/4}$. However, β_{el} is similar to β_{af}. In addition, the affine theory was adopted for the poly(dimethylsiloxane) network having a similar arm length and some entanglements ($M_n = 5600$).[25] Thus, we adopted hypothesis i.

Estimation of Loop Formation. As another topological inhomogeneity, loops have been known to be inevitable structures in model networks.[25] An elastically noneffective loop structure is defined as a circle-like structure containing the elastically noneffective or elastically redundant chain. An elastically noneffective loop structure has been vigorously discussed using the spanning tree model by Dusek et al.[26−28] If we accept the affine model and the Gaussian approximation of the configurational statistics of network chains, and assume that there is no entanglement, the difference between the ν and ν_{el} is attributed to the loop formation. The value of ν_{el}/ν was approximately 0.8 for all concentration regions. Using eq 10, the fraction of bonds wasted in elastically noneffective loop was estimated to 0.05, which is similar value expected in the spanning-tree theory. However, the spanning tree theory also expects that loops increase as ϕ_0 decreases.[25] In the Tetra-PEG gel system, the deviation between ν_{el} and ν was unchanged even when ϕ_0 decreased to below the ϕ^*, suggesting the opposite result, i.e., the near-absence of the loops. The reason for this discrepancy is not clear at this stage.

Although loops were not considered in the original tree-like model,[16] several theoretical approaches including the spanning-tree theory have been developed,.[28] Here, we propose the simple model treating the 'preloop' structure in order to show the superiority of the Tetra-PEG gel. If we assume the existence of preloop structure, we can estimate the probability that the small preloop structure formed from n sets of tetra-arm polymers become the elastically effective chains ($P(L_n)$) (Figure 5). For simplicity, we consider the case of tetra-arm polymers undergoing A−A type end-coupling and discuss the case of exclusive A−B type cross-end coupling. Here, we assume that (i) the number of preloops is too small to affect the original model, (ii) further intramolecular reaction does not occur, (iii) each functional group reacts equally. The $P(L_n)$ is estimated as the number of the EEC formed from the preloop structure normalized by the number of the EEC formed from the same number of individual polymers. For example, let us consider the case of preloop structures formed from three sets of tetra-arm polymers (L_3).

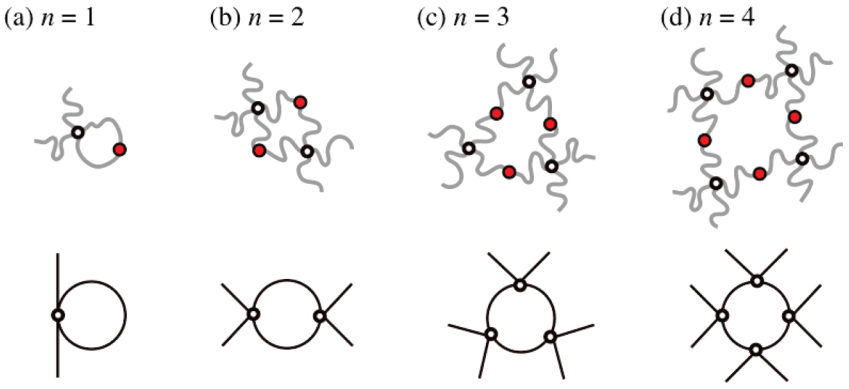

Figure 5. Preloop structures formed from n sets of tetra-arm polymers in A−A type of end coupling. The bottom panels represent the simplified pictures of preloop structure.

Figure 6 shows the connecting scheme of preloop (gray circle). Here, i number of lines outspreading from the circle represent the chains connected to the infinite network. Because the EEC is defined as the chains connecting the elastically effective cross-links, we can definitely evaluate the number of EEC. The dotted, thin, and bold lines represent the elastically noneffective chain, EEC between the preloop and the other polymer (EEC-I), and EEC in the preloop structure (EEC-II), respectively. We can calculate the number of EEC for each case; for example, in the case of the upper panel of $i = 3$, $^5/_2$ ($= 3 \times {}^1/_2 + 1 \times 1$) of EEC's are formed. By considering the number of situations, we can evaluate the $P(L_n)$ as a function of p. The calculated result for $n = 1, 2, 3, 4$ are represented as follows:

$$P(L_1) = 0 \tag{19}$$

$$P(L_2) = \frac{3}{2^4}C_3F_{out}(1-F_{out})^3 + 3_4C_4(1-F_{out})^4 \tag{20}$$

$$P(L_3) = \left(\frac{3}{2}12+\frac{9}{2}8\right)F_{out}{}^3(1-F_{out})^3 + (33+512)F_{out}{}^2(1-F_{out})^4 + \frac{11}{2}F_{out}(1-F_{out})^5 + 6(1-F_{out})^6 \tag{21}$$

$$P(L_4) = \left(\frac{3}{2}24+\frac{9}{2}32\right)F_{out}{}^5(1-F_{out})^3 + (3\times 6+5\times 48+6\times 16)F_{out}{}^4(1-F_{out})^4 + \left(\frac{11}{2}24+\frac{13}{2}32\right)F_{out}{}^3(1-F_{out})^5 + (6\times 4+7\times 24)F_{out}{}^2(1-F_{out})^6 + \frac{15}{2}F_{out}(1-F_{out})^7 + 8(1-F_{out})^8 \tag{22}$$

Figure 7 shows the calculation result of $P(L_n)$ as a function of p. Some important features appeared in Figure 7. First, L_1 never contributes to the elasticity, regardless of the p. Second, 1/4 of the chains are wasted in L_2 even when the reaction occurs stoichiometrically ($p = 1$). Third, when $n \geq 3$, all of the polymers in L_n contribute to the elasticity when the reaction is completed. Fourth, when $n \geq 3$, $P(L_n)$ is higher than that of individual single polymers at any conversion; in other words, EEC are formed more effectively from preloops than from individual modules. In the case of A-B type coupling between the bifunctional chain extender and the multifunctional cross-linker, L_1 and L_2 type of preloop structures are also formed. On the other hand, in the case of A−B type cross-end coupling between tetra-arm polymers, no L_1 is formed. In addition, only even-n of L_n are allowed in the case of A−B type cross-end coupling between tetra-arm polymers. Thus, a A-B type of cross-end coupling reaction using the tetra-arm polymers is expected to have fewer elastically noneffective loops than conventional ones, thus supporting our results.

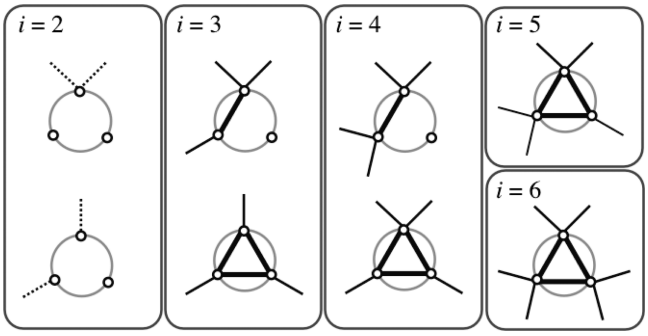

Figure 6. The preloop structures formed from three sets of tetra-arm polymers in the case that i number of arms are connected to the infinite network. The dotted, thin, and bold lines represent the elastically noneffective chain, EEC between the preloop and the other polymers, and EEC in the preloop structure.

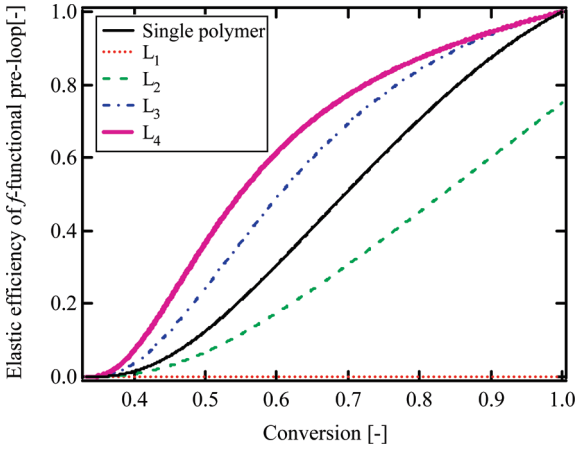

Figure 7. $P(L_n)$ as a function of p. The dotted, dashed, chain, bold, and thin lines represent the calculation result for $n = 1, 2, 3, 4$ of preloops and single polymer, respectively.

Estimation of Interpenetration. Here, we calculate the density of tetra-arm polymers and linear polymers. The gyration radius of a *f*-arm star polymer (R_{star}) is represented by

$$R_{star}^2 = \frac{3f-2}{f} R_{arm}^2 \quad (23)$$

where R_{arm} is the gyration radius of one arm.[29] The segment-number density of a polymer chain (ρ) scales as $\rho \sim N/R_g^3$, where N and R_g are the polymerization degree and the gyration radius of the polymer chains. We compare the tetra-arm polymer ($M_n = 2Nm_{EG}$) with the linear polymer ($M_n = Nm_{EG}$), where m_{EG} is the molecular weight of the monomeric unit of PEG. Ideally, these building blocks should form the same network structure. The ρ of the tetra-arm star polymer is 1.43 times larger than that of the linear polymer. Furthermore, according to the simulation of Freed et al., the interpenetration function, which indicates the excluded volume normalized by R_g^3, of the tetra-arm star polymer ($M_n = 2Nm_{EG}$), is two or three times larger than that of the linear polymer ($M_n = Nm_{EG}$),[30] also suggesting that the interpenetration between the tetra-arm star polymers is unlikely to occur.

Conclusion

We have investigated the topological defects in the Tetra-PEG gels formed from two symmetrical tetra-arm polymers by comparing the experimentally obtained mechanical moduli with the results of theoretical predictions based on the Miller-Macosko theory for polymer networks. The major findings of this study are as follows: (i) the reaction efficiency of Tetra-PEG gel was up to 75%; (ii) the elasticity of Tetra-PEG gel was well described by the affine theory; (iii) the formation of entanglements was negligible; and (iv) the fraction of bonds wasted in elastically noneffective loop was up to 0.05. The unique impenetrable sphere-like behavior of the tetra-arm star polymer in the semidilute solution as shown in our previous SANS experiment leads to the near-absence of topological defects, which contributes to the homogeneity of Tetra-PEG gel and to the resultant high mechanical strength.

References and Notes

(1) Shibayama, M. *Macromol. Chem. Phys.* **1998**, *199*, 1–30.
(2) Dusek, K. *Trends Polym, Sci,* **1997**, *5*, 268–274.
(3) Hild, G. *Prog. Polym. Sci.* **1998**, *23*, 1019–1149.
(4) Malkoch, M.; Vestberg, R.; Gupta, N.; Mespouille, L.; Dubois, P.; Mason, A. F.; Hedrick, J. L.; Liao, Q.; Frank, C. W.; Kingsbury, K.; Hawker, C. J. *Chem. Commun.* **2006**, *26*, 2774–2776.
(5) Durackova, A.; Valentova, H.; Duskova-Smrckova, M.; Dusek, K. *Polym. Bull.* **2007**, *58* (1), 201–211.
(6) Shibayama, M.; Takahashi, H.; Nomura, S. *Macromolecules* **1995**, *28*, 6860–6864.
(7) Villar, M. A.; Valles, E. M. *Macromolecules* **1996**, *29*, 4081–4089.
(8) Patel, S. K.; Malone, S.; Cohen, C.; Gillmor, J. R.; Colby, R. H. *Macromolecules* **1992**, *25*, 5241–5251.
(9) Sakai, T.; Matsunaga, T.; Yamamoto, Y.; Ito, C.; Yoshida, R.; Suzuki, S.; Sasaki, N.; Shibayama, M.; Chung, U. I. *Macromolecules* **2008**, *41*, 5379–5384.
(10) Matsunaga, T.; Sakai, T.; Akagi, Y.; Chung, U.; Shibayama, M. *Macromolecules* **2009**, *42*, 1344–1351.
(11) Matsunaga, T.; Sakai, T.; Akagi, Y.; Chung, U. I.; Shibayama, M. *Macromolecules* **2009**, *42*, 6245–6252.
(12) Bastide, J.; Leibler, L. *Macromolecules* **1988**, *21*, 2647–2649.
(13) Mendes, E.; Oeser, R.; Hayes, C.; Boue, F.; Bastide, J. *Macromolecules* **1996**, *29*, 5574–5584.
(14) Shibayama, M.; Shirotani, Y.; Shiwa, Y. *J. Chem. Phys.* **2000**, *112*, 442–449.
(15) de Gennes, P. G. *Scaling Concepts in Polymer Physics*, 1st ed.; Cornell University Press: Ithaca, NY, 1979.
(16) Miller, D. R.; Macosko, C. W. *Macromolecules* **1976**, *9*, 206–211.
(17) Treloar, L. R. G., *The Physics of Rubber Elasticity*; Clarendon: Oxford, U.K., 1975.
(18) Flory, P. J. *Proc. R. Soc. London, Ser. A: Math. Phys. Eng. Sci.* **1976**, *351* (1666), 351−380.
(19) Langley, N. R. Polmante.Ke. *J. Polym. Sci., Part B: Polym. Phys.* **1974**, *12* (6), 1023–1034.
(20) Gnanou, Y.; Hild, G.; Rempp, P. *Macromolecules* **1987**, *20*, 1662–1671.
(21) Urayama, K.; Kohjiya, S. *J. Chem. Phys.* **1996**, *104*, 3352–3359.
(22) Ferry, J. D., *Viscoelastic properties of polymers*; John Wiley and Sons: New York, 1980.
(23) Wool, R. P. *Macromolecules* **1993**, *26*, 1564–1569.
(24) Sperinde, J. J.; Griffith, L. G. *Macromolecules* **1997**, *30*, 5255–5264.
(25) Urayama, K.; Kawamura, T.; Kohjiya, S. *J. Chem. Phys.* **1996**, *105*, 4833–4840.
(26) Dusek, K.; Vojta, V. *Br. Polym. J.* **1977**, *9*, 164–171.
(27) Dusek, K.; Gordon, M.; Rossmurphy, S. B. *Macromolecules* **1978**, *11*, 236–245.
(28) Sarmoria, C.; Miller, D. R. *Comput. Theor. Polym. Sci.* **2001**, *11*, 113–127.
(29) Yamakawa, H., *Modern Theory of Polymer Solutions*; Harper & Row, Publishers, Inc.: New York, 1971.
(30) Miyake, A.; Freed, K. F. *Macromolecules* **1983**, *16*, 1228–1241.